Published in final edited form as:
Vis Neurosci. 2013 May ; 30(3): 55–64. doi:10.1017/S0952523813000096.

Loss of melanoregulin (MREG) enhances cathepsin-D secretion by the retinal pigment epithelium

Laura S. Frost[1], **Vanda S. Lopes**[2], **Frank P. Stefano**[1], **Alvina Bragin**[1], **David S. Williams**[2], **Claire H. Mitchell**[3], and **Kathleen Boesze-Battaglia**[1]

[1]Department of Biochemistry, School of Dental Medicine, University of Pennsylvania, Philadelphia, Pennsylvania

[2]Department of Ophthalmology and Neurobiology, Jules Stein Eye Institute, UCLA School of Medicine, Los Angeles, California

[3]Department of Anatomy and Cell Biology, School of Dental Medicine, University of Pennsylvania, Philadelphia, Pennsylvania

Abstract

Cathepsin-D (Cat-D) is a major proteolytic enzyme in phagocytic cells. In the retinal pigment epithelium (RPE), it is responsible for the daily degradation of photoreceptor outer segments (POSs) to maintain retinal homeostasis. Melanoregulin (MREG)-mediated loss of phagocytic capacity has been linked to diminished intracellular Cat-D activity. Here, we demonstrate that loss of MREG enhances the secretion of intermediate Cat-D (48 kDa), resulting in a net enhancement of extracellular Cat-D activity. These results suggest that MREG is required to maintain Cat-D homeostasis in the RPE and likely plays a protective role in retinal health. In this regard, in the *Mreg dsu/dsu* mouse, we observe increased basal laminin. Loss of the *Mreg* ^{dsu} allele is not lethal and therefore leads to slow age-dependent changes in the RPE. Thus, we propose that this model will allow us to study potential dysregulatory functions of Cat-D in retinal disease.

Keywords

Retinal pigment epithelium; Cathepsin-D processing; Phagocytosis; Protease secretion

Introduction

Most cells have the capacity to catabolize proteins and lipids through macroautophagy (Kon & Cuervo, 2010). Phagocytic cells have the additional burden of degrading the ingested material. In the retinal pigment epithelia (RPE), phagocytosis serves as a homeostatic regulator; in addition to the daily degradation of photoreceptor outer segment (POS) proteins, it is also responsible for the breakdown of POS-derived lipid components (Bazan et al., 2010; Kevany & Palczewski, 2010). Critical in the digestion of engulfed POS is the soluble lysosomal aspartic endopeptidase (EC 3.4.23.5) cathepsin-D (Cat-D) (Hayasaka, 1975; LaVail, 1978; LaVail, 1980; Besharse et al., 1998). Cat-D is synthesized in the rough endoplasmic reticulum as a pre-pro-enzyme and upon removal of the signal peptide forms a 52 kDa pro-Cat-D. Pro-Cat-D is targeted to intracellular structures including phagosomes, lysosomes, endosomes, and melanosomes (Hasilik & Neufeld, 1980; Kornfeld, 1990;

Address correspondence to: Kathleen Boesze-Battaglia, Department of Biochemistry, University of Pennsylvania, Philadelphia, PA 19104. battagli@upenn.edu.

Azarian et al., 2006), where the pro-peptide is cleaved resulting in a 48 kDa intermediate minimally active form. Further proteolytic cleavage yields the mature active protease which is composed of heavy (34 kDa) and light (14 kDa) chains linked by noncovalent interactions (Deguchi et al., 1994; Delbruck et al., 1994; Steinfeld et al., 2006).

Unlike other proteases, Cat-D retains dual functionality exhibiting both degradative and growth factor-like properties, involved in cell proliferation and angiogenesis (Vetvicka et al., 1994; Fusek & Vetvicka, 2005; Benes et al., 2008; Zaidi et al., 2008; Vetvicka & Vetvickova, 2011). Active forms of Cat-D can be released together with other proteases from lysosomes into the cytosol in response to apoptotic stimuli thus contributing to cell death. The dysregulated sorting and maturation of Cat-D are linked to progressive neurodegenerations, including retinal degeneration and Alzheimer's disease (Capurso et al., 2008; Haque et al., 2008; Urbanelli et al., 2008) as well as breast cancer metastasis (Garcia et al., 1996; Benes et al., 2008).

The toxic effects of defective Cat-D processing are most often progressive. For example, mice with loss of functional Cat-D develop progressive retinal atrophy over a 12-month period (Saftig et al., 1995). Transgenic mice that overexpress mutant minimally active Cat-D acquire features that resemble age-related retinal degenerative changes, including geographic atrophy, accelerated photoreceptor cell death, the presence of basal laminar deposits, and accumulation of POS breakdown products in the RPE (Rakoczy et al., 1996 *a*). Furthermore, up-regulation of normal Cat-D results in the secretion of unprocessed pro-Cat-D into the media (Rakoczy et al., 1996 *b*; Rakoczy et al., 1996 *c*; Rakoczy et al., 1997, 2002). Missense mutations in the human CTSD gene that result in minimally active Cat-D due to disrupted intracellular trafficking exhibit phenotypes characteristic of retinal degeneration and progressive psychomotor disability, further highlighting the progressive nature of Cat-D functional deficiency (Steinfeld et al., 2006). Cat-D maturation is highly regulated. Among the regulators is a newly described protein, melanoregulin (MREG) that is required for processing of active Cat-D. We have shown that defective Cat-D processing contributes to the accumulation of opsin positive phagosomes in the RPE of *Mreg dsu/dsu* mice (Damek-Poprawa et al., 2009). Concomitant with lack of Cat-D processing was the accumulation of retinal debris in the form of the lipofuscin component, pyridinium bisretinoid, A2E (Damek-Poprawa et al., 2009). We now extend those studies to determine consequences of MREG depletion on extracellular Cat-D levels. In these studies, we show that loss of MREG expression leads to the accumulation and basolateral secretion of immature Cat-D (46–48 kDa) both *in vivo* and *in vitro* (Damek-Poprawa et al., 2009). Secretion of the 46–48 kDa Cat-D is correlated with enhanced laminin in Bruch's membranes (BMs). Collectively, the *Mreg dsu/dsu* phenotype possess the hallmarks of retinal degenerations due to aging, including lipofuscin accumulation, delayed phagosome maturation, and basal laminar thickening and suggests a protective role for MREG against age-related degenerative eye disease.

Materials and methods

Materials and primer sets

Commercially available antibodies were purchased as follows: for Western blot analysis, goat anti-Cat-D and goat anti-Actin from Santa Cruz Biotechnology (Santa Cruz, CA), rabbit anti-MREG from Abnova (Taipei City, Taipei), rabbit antigoat and goat antirabbit horseradish peroxidase-conjugated secondary antibody from Thermo Scientific (Rockford, IL). For immunofluorescence analysis, we used mouse anti-MREG from Novus Biologicals (Littleton, CO) and rabbit antilaminin (Sigma-Aldrich). Secondary antibodies were Alexa-Fluor 594 donkey antirabbit and Alexa-Fluor 488 donkey antimouse from Invitrogen (Grand Island, NY). For double-labeling in immune-electron microscopy, we used a polyclonal Cat-

D antibody from Dr. Dean Bok (Bosch et al., 1993) and mouse mAb anti-MREG 165 (Boesze-Battaglia et al., 2007). The polyclonal Cat-D antibody was also used in immunohistochemistry (IHC) analysis of *Mreg* $^{dsu/dsu}$ and *Mreg* $^{+/+}$ eyecups. The following *Mreg* primers were used in these studies, hMREG, 5′-TTTGGAGCAACTCTGGTGAGGGAT-3′ (forward) and 5′-GTGCAATGAGACGGTCCACAACAA-3′ (reverse).

Cell culture

ARPE-19 cells (ATCC, CRL-2302) were grown in Dulbecco's modified Eagle medium (DMEM) supplemented with 10% fetal calf serum as described (Ahmado et al., 2011). For secretion experiments, shRNA-treated (MREG or nontarget control) ARPE-19 cells were grown as described (Dunn et al., 1996). Cells in suspension (0.5 ml) were added to the upper chamber of a 12-well plate, containing polycarbonate Transwell inserts, with a 3.0-m-pore diameter (Costar, Corning, NY). They were maintained in the growth medium (GM) containing DMEM (high glucose) supplemented with 1% fetal bovine serum (FBS). Cells were cultured until confluent colonies were present. Cells were then maintained at 37°C/5% CO_2 for analysis. Media were collected from the basal chamber for analysis. Trans epithelial resistance was routinely 45–48 ohms/cm^2.

Primary RPE cell culture

Primary RPE cells were isolated from *Mreg* $^{dsu/dsu}$ and *Mreg* $^{+/+}$ (C57BL6/J) mice at 6 weeks old and cultured as described (Gibbs et al., 2003). Briefly, intact eyes were removed and lots of 10–12 eyes were washed twice in 5 ml DMEM containing high glucose, then incubated with 5 ml of 2% (w/v) Dispase in DMEM for 45 min at 37°C. Eyes were washed twice in the GM. Posterior eyecups were isolated and incubated in the GM for 20 min at 37°C to facilitate separation of the neural retina from the RPE. The neural retina was removed and intact sheets of RPE cells were peeled off the underlying basement membrane (BM) and transferred into a sterile 60-mm culture dish, containing 5 ml of the fresh GM. The sheets of RPE were washed three times with GM, twice with Ca^{+2} and Mg^{+2} free Hanks' balanced salt solution (5 mM KCl, 0.5 mM KH_2PO_4, 4 mM $NaHCO_3$, 150 mM $NaCl_3$ mM, $Na_2HPO_4 7H_2O$ 5 mM glucose, pH 7.4) and briefly triturated by using a fine point Pasteur pipette. RPE cells were sedimented by centrifugation at 200 × *g* for 5 min and resuspended in the GM to a final concentration of 50,000 cells per ml and plated. Cells in suspension (0.5 ml) were plated on Transwell plates (Corning Costar, Corning, NY) using 12-mm diameter inserts with 0.4 μm pores on polyester membranes (Thermo-Fisher Scientific, Pittsburgh, PA) and maintained as described above.

Lentiviral shRNA transduction

ARPE-19 cells were passaged and subsequently (within 24 h) transduced with MISSION shRNA lentiviral particles (Sigma-Aldrich, St. Louis, MO) with a multiplicity of infection (MOI) of five in the presence of 8 μg/ml hexadimethrine bromide and incubated at 37°C for 18–20 h (Zufferey, 1997; Stewart et al., 2003). Fresh media were added and cells incubated overnight. Media were then replaced with media containing 2 μg/ml puromycin for selection purposes and changed every 3–4 days until resistant colonies could be identified. Control cells were transduced with pLKO.1-puro shRNA control particles containing no shRNA insert (C1) or nontarget (nonhuman) shRNA insert (C2). MREG knockdown cells were transduced with Mreg shRNA lentiviral particles, clone IDs TRCN0000133942, TRCN0000134116, TRCN0000134266, TRCN0000134495, TRCN0000134842 (Sigma-Aldrich), designated M1-M5, respectively. Knockdown of the *Mreg*^{dsu} gene was confirmed by agarose gel with products from real-time polymerase chain reaction (RT-PCR) and of MREG protein by Western blot analysis.

Animals

Melanoregulin is the product of the *Mreg*^{dsu} gene locus [previously known as dilute suppressor (dsu)- or whn-dependent transcript 2 (wdt2)]. *Mregdsu/dsu* mice carry the *Mreg dsu* allele (mouse accession number, Q6NV65) in which deletion of the first two exons results in an effective null allele (O'Sullivan et al., 2004). *Mreg*$^{-/-}$ mice (on C57BL6/J genetic background) used in these studies were originally maintained and propagated at the NCI, National Institutes of Health, and were generous gifts from Drs. Jenkins and Copeland (Texas Medical Center). Both *Mreg*^{dsudsu} and *Mreg*$^{++}$(C57BL/J6 genetic background, obtained from the Jackson Laboratory) mice were housed under cyclic light conditions: 12-h light/12-h dark and fed *ad libitum*. All procedures involving animals were approved by the University of Pennsylvania, Institutional Animal Care and Use Committee and were in accordance with the Association for Research in Vision and Ophthalmology guidelines for use of animals.

Immunoblotting

Cleared RPE lysates were prepared as described (Damek-Poprawa et al., 2009). Briefly, ARPE-19 or primary RPE cells were lysed in cell lysis buffer containing 20 mM Tris–HCl (pH 7.5), 150 mM NaCl, 1 mM Na_2 EDTA, 1 mM EGTA, 1% Triton, 2.5 mM sodium pyrophos-phate, 1 mM beta-glycerophosphate, 1 mM Na_3 VO 4, 1 μ g/ml leupeptin (Cell Signaling, Danvers, MA) and protease inhibitor cocktail (Roche, Nutley, NJ) and centrifuged at 13,500 rpm for 15 min at 4°C. Protein concentrations were determined using a BioRad assay. Conditioned media isolated form the basolateral chamber were also centrifuged at 13,500 rpm for 15 min at 4°C and supernatant collected prior to analysis. Conditioned media and protein lysates were loaded in each lane in sample buffer (2% SDS, 10% glycerol, 0.001% bromophenol blue, and 0.05 m Tris-HCl, pH 6.8), separated on 4–12% SDS–PAGE (Invitrogen) under reducing conditions and to transferred nitrocellulose using an iBlot system (Invitrogen). Blots were probed with anti-Cat-D (1:500) or anti-MREG (1:500) or anti-Actin (1:500) antibody. Appropriate horseradish peroxidase-conjugated secondary antibodies were subsequently used for detection. β-actin (Santa Cruz) was used as a loading control. Visualization of the primary antibody was performed by incubating membranes with the corresponding peroxidase-conjugated secondary antibody (1:4500; Thermo Scientific) for 1 h at room temperature. Blots were developed by enhanced chemiluminescence (ECL-West-Pico) (Thermo Scientific) either on a film or captured on ImageQuant™ LAS 400 image reader (GE Healthcare, Mickleton, NJ). Immunoblots were scanned and relative band density was determined using ImageJ v1.34 software.

Cat-D activity

Cat-D activity was measured in conditioned media from shRNA Control (C2) and MREG (M5) using a fluorogenic substrate according to the manufacturer's protocol (Sigma-Aldrich) and our previous studies (Damek-Poprawa et al., 2009). The substrate is a fluorogenic decapeptide, MCAc–Gly–Lys–Pro–Ile–Leu–Phe–Phe–Arg–Leu–Lys–(Dnp)D–Arg–NH2, in which MCA is quenched by DNP. Upon proteolytic cleavage by Cat-D, the substrate is dequenched, and MCA peptide fluorescence is followed over time. Substrate was added to the samples at a final concentration of 20 μ M, and fluorescence (λ_{ex} = 328 nm, λ_{em} = 393 nm) was followed for 30 min at 37°C at 2-min intervals. The fluorescence of 1.0 nmol of the fluorogenic substrate was determined from a standard curve using known concentrations of MCA peptide. The Cat-D activity of each sample was calculated using the following equation;

$$\text{Units/ml} = \Delta F/T \times D/V_{\text{enz}} \times 1/F\,(1 \quad \text{nmol})\,,$$

where ΔF = increase in fluorescence during the time period of linearity in fluorescence measurement; T = time (min), when increase in fluorescence is linear; D = dilution factor of enzyme sample; V_{enz} = volume of enzyme sample (ml); F (1 nmol) = fluorescence of 1 nmol of fluorogenic substrate. One unit of activity is defined as nmol of MCA peptide release per min per ml of enzyme sample. Activities were normalized to the amount of secreted Cat-D determined by immunoblot.

LDH cytotoxicity assay

Cell membrane integrity was determined by measuring lactate dehydrogenase (LDH) activity released into the culture medium using an assay kit (Cayman Chemical, Ann Arbor, MI). Here LDH catalyzes the reduction of NAD+ to NADH and H+ by oxidation of lactate to pyruvate. In the second step of the reaction, diaphorase uses the NADH and H+ formed to catalyze the reduction of a tetrazolium salt (INT) to formazan, which absorbs strongly at 490–520 nm. The amount of formazan produced is proportional to the amount of LDH released into the culture media as a result of cytotoxity or cell lysis. LDH activity was measured in conditioned media from C2 and M5 cells up to 10 days in culture as formazan produced detected at 492 nm using an automated microplate reader. The amount of LDH was calculated using linear regression of the LDH standard curve. One unit of activity was defined as the amount of LDH that catalyzes the reaction of 1 μ mol of substrate/min.

Gel RT-PCR analysis

RNA was isolated using Qiagen RNeasy Mini Kit (Valencia, CA) and yield determined by measuring absorbance at 260 nm (Gee et al., 2006). 1 μ g of total RNA was converted into cDNA using superscipt first strand synthesis system for RT-PCR (Invitrogen). PCR amplification for gel PCR analysis was performed using PCR mastermix solution (Sigma-Aldrich) and primers specific for human MREG and glyceraldehyde-3-phosphate (GAPDH) used as an endogenous control. cDNA samples were run on 1% agarose gels containing ethidium bromide and imaged under UV light.

Confocal microscopy

Immunohistochemistry was performed on frozen sections of 6- and 18-month-old mouse retinas (Boesze-Battaglia et al., 2007). Eyecups were fixed in 4% paraformaldehyde in PBS (pH 7.4) over-night at 4°C, cryoprotected in 30% sucrose, and embedded in OCT. The 7 μ m sections were successively stained with antilaminin (1:100) followed by secondary antibody, Alexa 594 donkey–antirabbit (1:500), followed by Alexa Fluor 488 phalloidin (1:100). In parallel studies, sections were stained with anti-Cat-D (1:100) followed by Alexa 555 antirabbit secondary antibody (1:1000). Controls were incubated with secondary antibodies only. Nuclei were visualized with Hoechst 33258. Images were captured on a Nikon A1R live cell confocal imaging system. Data were analyzed using Nikon Elements AR Software ver.3.2

Immunoelectron microscopy

Ultrathin sections for transmission electron microscopy were obtained from LR White-embedded mouse (*Mreg*$^{+/+}$) retinas. They were double-labeled with Cat-D and MREG antibodies, generated in rabbit and mouse, respectively (see above). Rabbit IgG antibodies, conjugated to 15-nm gold particles, and mouse IgG antibodies, conjugated to 10-nm gold particles, were used as secondary antibodies.

Statistical analyses

Data were analyzed using SigmaStat version 3.1. Data are reported as mean ± s.d. or SEM as indicated. Statistical analysis used a oneway ANOVA Dunn's test, results with $P < 0.05$ were considered significant.

Results

MREG co-localizes with the aspartyl protease, Cat-D in degradative compartments

Our previous studies documenting reduced Cat-D activity with the subsequent accumulation of lipofuscin in aged RPE cells isolated from *Mreg-/-* mice, suggest a protective role for MREG in maintaining RPE health. Although MREG is known to be associated with small intracellular vesicles, its distribution profile relative to Cat-D is unknown. Therefore, in order to decipher the relationship between MREG function and Cat-D processing, we analyzed the distribution profile of MREG and Cat-D in RPE cells by Immuno-EM. Cat-D and MREG were both abundant in lysosomes and to a lesser extent in phagosomes (Fig. 1A and 1B). MREG was also localized to melanosomes (Fig. 1C and 1D) consistent with its putative role as a cargo receptor on these organelles (Damek-Poprawa et al., 2009; Ohbayashi et al., 2012; Rachel et al., 2012).

Mreg knockdown leads to aberrant secretion of Cat-D (48 kDa)

To determine the effect of diminished MREG expression on the disposition of Cat-D, we generated several stable ARPE19 MREG knockdown cell lines using shRNA lentiviral particles. The gene silencing efficiency from five different clones designated M1-M5 (Sigma-Aldrich) was analyzed by agarose gel RT-PCR (Fig. 2A) and western blotting (Fig. 2B). MREG protein knockdown varied from none (M1) to <60% (M2) to over 90% knockdown in M5 cells (Fig. 2C). In these studies, we used M5 (MREG knockdown) and C2 (nontarget shRNA) as a control (Fig. 2D). MREG expression in control cells (C2) was further confirmed as the appearance of intracellular MREG positive puncta, with almost a complete absence of these structures in the M5 clone (Fig. 2E).

It is well documented that defective Cat-D processing leads to its mis-sorting and nonspecific secretion in MCF-7 cells (Capony et al., 1994; Kokkonen et al., 2004), Human umbilical vein endothelial cells (HUVEC), and endothelial cells types (Erdmann et al., 2008). To determine if this was the case in the absence of MREG, we analyzed extracellular Cat-D from M5 and C2 ARPE19 cells. ARPE19 cells were cultured for up to 21 days and basolateral conditioned media analyzed for Cat-D levels and activity on day 7, 10, 15, and 21. MREG knockdown (M5) cells exhibited increased secretion of the 48 kDa, intermediate form of Cat-D. Within 10 days, there was a 40% increase in secreted Cat-D with subsequently more Cat-D secreted by 15 and 21 days (Fig. 3A). Increased Cat-D secretion was also observed in C2 control cells albeit to a lesser extent than in M5. Similar results were obtained with RPE-J cells using a rat-specific shRNA (data not shown). The increase in Cat-D in the C2 cells is not entirely unexpected, given the extensive secretion of Cat-D in transgenic mice (Rakoczy et al., 1996 *a*). The increase in Cat-D secretion by the M5 cells was not due to increased cell lysis since there was no change in LDH release between C2 and M5 cells (Table 1). Furthermore, loss of MREG did not alter Cat-D mRNA levels in either the $Mreg^{dsu/dsu}$ RPE (Damek-Poprawa et al., 2009) or the M5 cells (data not shown).

To determine if the secreted Cat-D had activity, fluorogenic substrates were used to quantify activity of the secreted Cat-D. Based on the size of the secreted enzyme, 48 kDa (Fig. 3A) and activity levels (Fig. 3B), we suggest that the isolated Cat-D variant is not the inactive pro-enzyme but an intermediate (minimally active) form of Cat-D. Activity of the secreted Cat-D was increased upon MREG depletion (Fig. 3B), however, when normalized to the

levels of Cat-D protein, this increase was only moderately significant at days 10 and 15 (Table 2).

Missorting and incomplete maturation of Cat-D is associated with neurodegenerative disorders characterized by lipofuscinosis (Woessner, 1977; Koike et al., 2003; Siintola et al., 2006). In the *Mreg*$^{dsu/dsu}$ mouse, concomitant with lack of Cat-D processing, there was accumulation of retinal debris in the form of lipofuscin (Damek-Poprawa et al., 2009). To correlate our *in vitro* results with the *Mreg*$^{dsu/dsu}$ mouse model, we analyzed Cat-D distribution in RPE cells and secretion from cultures of primary RPE cells isolated from *Mregdsu/dsu* and *Mreg*$^{+/+}$ mice. Cat-D positive puncta were observed in RPE from both mice. However, there was substantially more Cat-D containing puncta and aggregates in the *Mregdsu/dsu* mice (Fig. 3C). Furthermore, when RPE cells from these mice were cultured and Cat-D secretion measured over a 10-day period, an almost twofold increase in pro-Cat-D secretion was observed (Fig. 3D, Western blot inset). Loss of MREG results in increased laminin deposits in the BM by IHC.

In the RPE, accumulation of Cat-D results in features that resemble age-related retinal degenerative changes including the presence of basal laminar deposits and accumulation of POS breakdown products. We have already observed an accumulation of POS breakdown products as well as defective Cat-D processing in RPE devoid of MREG. In this next study, we sought to determine if the stability of the RPE–BM interface was compromised with the excessive secretion of Cat-D by assessing laminin in BM and choroid. Laminin was found to be localized to the choroid and BM of both *Mreg*$^{dsu/dsu}$ and *Mreg*$^{+/+}$ mice (Fig. 4A). Quantification of the intensity of laminin in these two regions (Erdmann et al., 2008) showed an enhancement of laminin in the *Mreg*$^{dsu/dsu}$ mice when compared with *Mreg*$^{+/+}$ mice in BM (Fig. 4B) as early as 6 months of age, with a statistically significant increase in laminin levels in the *Mreg*$^{dsu/dsu}$ retinas [relative mean fluorescence intensity (ROI), 1008. 335 ± 159.6 and 424.50 ± 82.3 with $P<05$, respectively]. Laminin staining remained elevated in the *Mreg*$^{dsu/dsu}$BM at 18 months old with an ROI of 715.63 ± 196.19, compared with *Mreg*$^{+/+}$ mice 211.45 ± 6.10 ($P<05$).

Discussion

The involvement of minimally processed Cat-D in the pathogenesis of metastatic breast and prostate cancer, neurodegenerative disease as well as retinal degeneration seen in age-related macular degeneration (AMD) is well documented (Woessner, 1977; Rakoczy et al., 1996 *a*; Koike et al., 2003; Siintola et al., 2006). In these studies, we further describe a novel regulator of Cat-D processing, a small intracellular protein called MREG. This protein appears to be required for the efficient processing of Cat-D; loss of MREG is linked to decreased intracellular mature (34 kDa) Cat-D activity as well as the accumulation of Cat-D substrate in the RPE (Damek-Poprawa et al., 2009). In this study, we explore the disposition of Cat-D in the extracellular media, we demonstrate that a minimally processed 48 kDa form of Cat-D is secreted in RPE cells devoid of MREG, concomitant with this secretion is an increase in extra cellular matrix (ECM) proteins, specifically, laminin and an apparent thickening of BM.

The relationship between loss of MREG function and Cat-D dysfunction and Cat-D secretion in the *Mreg*$^{dsu/dsu}$ mouse and age-related pathological changes are particularly relevant to our understanding of RPE health given the rapidly accumulating evidence suggesting that age-associated progressive retinal dystrophy is a multifactorial disease with numerous environmental stressors contributing to the pathology (Tikellis et al., 2007; Kanda et al., 2008). The metabolic demands on the RPE alone are considerable and further exacerbated by their location in the highly oxygenated environment of the outer retina and

their exposure to light (Delcourt et al., 1999; Cai et al., 2000; Zarbin, 2004; Kanda et al., 2008) and references therein. Environmental and metabolic factors are known to re-program protein sorting and processing decisions in disease models (Rakoczy et al. 1996 *a*; Haque et al., 2008; Hu et al., 2008; Khalkhali-Ellis et al., 2008; Zaidi et al., 2008). A similar paradigm may contribute to RPE dysfunction due to altered lysosomal hydrolase trafficking and sorting as illustrated best by Cat-D. Although the main physiological house-keeping role of Cat-D is protein turnover, in pathogenic lesions, Cat-D actively degrades proteins, boosts inflammatory responses and thereby may promote the initiation or advancement of blinding diseases (Rakoczy et al. 1996 *a*; Haque et al., 2008; Hu et al., 2008; Khalkhali-Ellis et al., 2008; Zaidi et al., 2008). The critical change that converts Cat-D from a physiological to a pathological player is not known although several lines of evidence suggest that stress-mediated protein missorting of trafficking proteins plays a role in the switch. For example, uptake of oxidized-LDL (low density lipoprotein) results in diminished Cat-D maturation with subsequent secretion of Cat-D into the ECM (Hoppe et al., 2001, 2004 *a*, b). Treatment of primary cultures with oxidized LDLs impairs intracellular Cat-D trafficking (Hoppe et al., 2001) and alters MREG levels (Frost, 2011).

The pathogenic impact of improperly processed inactive or minimally active Cat-D occurs both intracellularly and extracellularly, thereby affecting RPE as well as BM and choroid health. Intracellular Cat-D regulates cholesterol efflux from LE/Lys-mediated by the ATP-binding cassette protein ABCA1, a cholesterol transporter. This observation is of particular relevance to our studies because allelic variants of ABCA1 have recently been associated with susceptibility to AMD (Zareparsi et al., 2005; Tikellis et al., 2007). In addition, cholesterol and cholesteryl ester deposits are observed beneath the RPE in AMD thus implicating abnormal cholesterol trafficking regulated by Cat-D in disease progression (Malek et al., 2003; Li et al., 2005). In our own studies, MREG-mediated loss of Cat-D activity resulted in delayed phagosome maturation which over time (18 month old mice) lead to lipofuscinosis in these mice (Damek-Poprawa et al., 2009). Transgenic mice overexpressing inactive Cat-D show a similar phagosome accumulation as well as age-dependent photoreceptor degeneration (Rakoczy et al., 2002). The secretion of either unprocessed or minimally active Cat-D is also expected to shift the balance of RPE-BM-choroid health over time. For example, transgenic mice expressing nonfunctional Cat-D develop retinal abnormalities that resemble age-related macular degenerative changes including basal laminar deposits (Rakoczy et al., 2002). In the studies presented here, increased laminin staining indicative of BM thickening was observed in aging *Mreg*$^{dsu/dsu}$ mice.

On a molecular level, the generation of active Cat-D involves several posttranslational modifications; Cat-D is expressed in a full-length inactive form (52 kDa) which then undergoes a series of proteolytic processing steps to produce an active 34 kDa form (Deguchi et al., 1994; Delbruck et al., 1994; Zaidi et al., 2008). In the inactive Cat-D transgenic mouse, there was a subsequent elevation of Cat-S (Rakoczy et al., 2002). Whether elevated Cat-S in our *in vitro* studies could represents a compensatory mechanism or is due to lysosome alkalinization secondary to the accumulation of debris due to large amounts of minimally active Cat-D is unknown (Damek-Poprawa et al., 2009). Similar *in vitro* studies are underway in which A2E is added to C2 and M5 cultures to help to clarify this relationship.

The molecular mechanism by which diminished MREG may contribute to increased Cat-D secretion while speculative likely involves the newly described role of MREG as a cargo receptor for dynein-dependent processes (Ohbayashi et al., 2012). Cat-D maturation in the *Mregdsu/dsu* RPE may be affected by the inefficient retrograde trafficking of intermediate transport vesicles to the perinuclear region of the cell where lysosomes are typically

abundant. Secretory lysosomes are commonly found in cells of hematopoietic lineage with exceptions including pigmented cells and contain the relevant degradative proteins. ARPE19 cells, for example, release Fas ligand-containing microvesicles derived from secretory lysosomes (McKechnie et al., 2006). In the absence of MREG, we propose that lysosome-related organelles including secretory ly-sosomes may be enhanced and proteases secreted (Blott & Griffiths, 2002). Furthermore, we have shown that loss of MREG function facilitates an increase in the size of micromelanosomes in the choroid of the HPS BLOC-2 mutants ruby, ruby2, and cocoa, while a transgenic mouse overexpressing melanoregulin corrects the size of RPE macromelanosomes in Oa1(ko/ko) mice. Collectively, these results suggest that MREG levels regulate aspects of the enzymatic machinary involved in melanosomogenesis (Rachel et al., 2012). Herein, we propose that one aspect of loss of MREG function is enhanced secretion of CatD containing lysosomes.

Collectively, these studies, in combination with our previously published work, suggest that the *Mregdsu/dsu* mouse is a viable model in which to understand the implications of age-related changes in RPE degradative function. Because loss of the $Mreg^{dsu}$ allele is not lethal, it leads to slow age-dependent changes in RPE and has the potential to allow us to differentiate between the housekeeping and pathogenic functions of Cat-D. In summary, these studies suggest that loss of function $Mreg^{dsu}$ gene mutations may confer enhanced susceptibility to age-related retinal degenerative diseases, either due to specific genetic abnormalities or due to environmental stressors.

Acknowledgments

We would like to thank the SDM-live cell-imaging core for data analysis, Dr. Nancy Philp for her critical reading of the manuscript and insight into retinal pathology, and Dr. Alan Laties for helpful discussions. This work was supported by NIH grant R01 EY010420 and R21EY018705 to KBB, R01 EY013434 to CHM, Vision Research Core Grant EY001583 (KBB and CHM), and R01 EY07042 to DSW. DSW is an RPB Jules and Doris Stein Professor.

References

Ahmado A, Carr AJ, Vugler AA, Semo M, Gias C, Lawrence JM, Chen LL, Chen FK, Turowski P, da Cruz L, Coffey PJ. Induction of differentiation by pyruvate and DMEM in the human retinal pigment epithelium cell line ARPE-19. Investigative Ophthalmology and Visual Science. 2011; 52:7148–7159. [PubMed: 21743014]

Azarian S, McLeod I, Lillo C, Gibbs D, Yates JR, Williams DS. Proteomic analysis of mature melanosomes from the retinal pigment epithelium. Journal of Proteomic Research. 2006; 5:521–529.

Bazan NG, Calandria JM, Serhan CN. Rescue and repair during photoreceptor cell renewal mediated by docosahexaenoic acid-derived neuroprotectin D1. Journal of Lipid Research. 2010; 51:2018–2031. [PubMed: 20382842]

Benes P, Vetvicka V, Fusek M. Cathepsin D: Many functions of one aspartic protease. Critical Reviews in Oncology/Hematology. 2008; 68:12–28. [PubMed: 18396408]

Besharse, JC.; DeFoe, DM.; Marmor, MF.; Wolfensberger, TJ. Role of the retinal pigment epithelium in photoreceptor membrane turnover. In: Besharse, JC., editor. The Retinal Pigment Epithelium. Vol. 8. Oxford University Press; New York: 1998. p. 152

Blott EJ, Griffiths GM. Secretory lysosomes. Nature. 2002; 3:122–131.

Boesze-Battaglia K, Song H, Sokolov M, Lillo C, Pankoski-Walker L, Gretzula C, Gallagher B, Rachel RA, Jenkins NA, Copeland NG, Morris F, Jacob J, Yeagle P, Williams DS, Damek-Poprawa M. The tetraspanin protein peripherin-2 forms a complex with melanoregulin, a putative membrane fusion regulator. Biochemistry. 2007; 46:1256–1272. [PubMed: 17260955]

Bosch E, Horwitz J, Bok D. Phagocytosis of outer segments by retinal pigment epithelium: Phagosome-lysosome interaction. The Journal of Histochemistry and Cytochemistry. 1993; 41:253. [PubMed: 8419462]

Cai J, Nelson KC, Wu M, Sternberg P Jr. Jones DP. Oxidative damage and protection of the RPE. Progress in Retinal and Eye Research. 2000; 19:205–221. [PubMed: 10674708]

Capony F, Braulke T, Rougeot C, Roux S, Montcourrier P, Rochefort H. Specific mannose-6-phosphate receptor-independent sorting of pro-cathepsin D in breast cancer cells. Experimental Cell Research. 1994; 215:154–163. [PubMed: 7957663]

Capurso C, Solfrizzi V, D'Introno A, Colacicco AM, Capurso SA, Bifaro L, Menga R, Santamato A, Seripa D, Pilotto A, Capurso A, Panza F. Short arm of chromosome 11 and sporadic Alzheimer's disease: Catalase and cathepsin D gene polymorphisms. Neuroscience Letters. 2008; 432:237–242. [PubMed: 18248894]

Damek-Poprawa M, Diemer T, Lopes VS, Lillo C, Harper DC, Marks MS, Wu Y, Sparrow JR, Rachel RA, Williams DS, Boesze-Battaglia K. Melanoregulin (MREG) modulates lysosome function in pigment epithelial cells. The Journal of Biological Chemistry. 2009; 284:10877–10889. [PubMed: 19240024]

Deguchi J, Yamamoto A, Yoshimori T, Sugasawa K, Moriyama Y, Futai M, Suzuki T, Kato K, Uyama M, Tashiro Y. Acidification of phagosomes and degradation of rod outer segments in rat retinal pigment epithelium. Investigative Ophthalmology and Visual Science. 1994; 35:568–579. [PubMed: 8113008]

Delbruck R, Desel C, von Figura K, Hille-Rehfeld A. Proteolytic processing of cathepsin D in prelysosomal organelles. European Journal of Cell Biology. 1994; 64:7–14. [PubMed: 7957314]

Delcourt C, Cristol JP, Leger CL, Descomps B, Papoz L. Associations of antioxidant enzymes with cataract and age-related macular degeneration. The POLA Study. Pathologies Oculaires Liées à l'Age. Ophthalmology. 1999; 106:215–222. [PubMed: 9951468]

Dunn KC, Aotaki-Keen AE, Putkey FR, Hjelmel LM. ARPE-19, a human retinal pigment epithelial cell line with differentiated properties. Experimental Eye Research. 1996; 62:155–169. [PubMed: 8698076]

Erdmann S, Ricken A, Hummitzsch K, Merkwitz C, Schliebe N, Gaunitz F, Strotmann R, Spanel-Borowski K. Inflammatory cytokines increase extracellular procathepsin D in permanent and primary endothelial cell cultures. European Journal of Cell Biology. 2008; 87:311–323. [PubMed: 18387691]

Fusek M, Vetvicka V. Dual role of cathepsin D: Ligand and protease. Biomedical papers of the Medical Faculty of the University Palacký, Olomouc, Czechoslovakia. 2005; 149:43–50.

Garcia M, Platet N, Liaudet E, Laurent V, Derocq D, Brouillet JP, Rochefort H. Biological and clinical significance of cathepsin D in breast cancer metastasis. Stem Cells. 1996; 14:642–650. [PubMed: 8948022]

Gee K, Angel JB, Ma W, Mishra S, Gajanayaka N, Parato K, Kumar A. Intracellular HIV-Tat expression induces IL-10 synthesis by the CREB-1 transcription factor through Ser133 phosphorylation and its regulation by the ERK1/2 MAPK in human monocytic cells. The Journal of Biological Chemistry. 2006; 281:31647–31658. [PubMed: 16920714]

Gibbs D, Kitamoto J, Williams DS. Abnormal phagocytosis by retinal pigmented epithelium that lacks myosin VIIa, the Usher syndrome 1B protein. Proceedings of the National Academy of Sciences of the United States of America. 2003; 100:6481–6486. [PubMed: 12743369]

Haque A, Banik NL, Ray SK. New insights into the roles of endolysosomal cathepsins in the pathogenesis of Alzheimer's disease: Cathepsin inhibitors as potential therapeutics. CNS & Neurological Disorders Drug Targets. 2008; 7:270–277. [PubMed: 18673211]

Hasilik A, Neufeld EF. Biosynthesis of lysosomal enzymes in fibroblasts. Synthesis as precursors of higher molecular weight. The Journal of Biological Chemistry. 1980; 255:4937–4945. [PubMed: 6989821]

Hayasaka S, Hsa MK. Degradation of rod outer segment proteins by cathepsin D. The Journal of Biological Chemistry. 1975; 78:1365–1367.

Hoppe G, Marmorstein AD, Pennock EA, Hoff HF. Oxidized low density lipoprotein-induced inhibition of processing of photoreceptor outer segments by RPE. Investigative Ophthalmology and Visual Science. 2001; 42:2714–2720. [PubMed: 11581220]

Hoppe G, O'Neil J, Hoff HF, Sears J. Accumulation of oxidized lipid-protein complexes alters phagosome maturation in retinal pigment epithelium. Cellular and Molecular Life Sciences: CMLS. 2004a; 61:1664–1674. [PubMed: 15224189]

Hoppe G, O'Neil J, Hoff HF, Sears J. Products of lipid peroxidation induce missorting of the principal lysosomal protease in retinal pigment epithelium. Biochim Biophys Acta. 2004b; 1689:33–41. [PubMed: 15158911]

Hu L, Roth JM, Brooks P, Luty J, Karpatkin S. Thrombin up-regulates cathepsin D which enhances angiogenesis, growth, and metastasis. Cancer Research. 2008; 68:4666–4673. [PubMed: 18559512]

Kanda A, Abecasis G, Swaroop A. Inflammation in the pathogenesis of age-related macular degeneration. The British Journal of Ophthalmology. 2008; 92:448–450. [PubMed: 18369057]

Kevany BM, Palczewski K. Phagocytosis of retinal rod and cone photoreceptors. Physiology. 2010; 25:8–15. [PubMed: 20134024]

Khalkhali-Ellis Z, Abbott DE, Bailey CM, Goossens W, Margaryan NV, Gluck SL, Reuveni M, Hendrix MJ. IFN-gamma regulation of vacuolar pH, cathepsin D processing and autophagy in mammary epithelial cells. Journal of Cellular Biochemistry. 2008; 105:208–218. [PubMed: 18494001]

Koike M, Shibata M, Ohsawa Y, Nakanishi H, Koga T, Kametaka S, Waguri S, Momoi T, Kominami E, Peters C, Figura K, Saftig P, Uchiyama Y. Involvement of two different cell death pathways in retinal atrophy of cathepsin D-deficient mice. Molecular and Cellular Neurosciences. 2003; 22:146–161. [PubMed: 12676526]

Kokkonen N, Rivinoja A, Kauppila A, Suokas M, Kellokumpu I, Kellokumpu S. Defective acidification of intracellular organelles results in aberrant secretion of cathepsin D in cancer cells. The Journal of Biological Chemistry. 2004; 279:39982–39988. [PubMed: 15258139]

Kon M, Cuervo AM. Chaperone-mediated autophagy in health and disease. FEBS Letters. 2010; 584:1399–1404. [PubMed: 20026330]

Kornfeld S. Lysosomal enzyme targeting. Biochemical Society Transactions. 1990; 18:367–374. [PubMed: 2164980]

LaVail MM. The retinal pigment epithelium in mice and rats with inherited retinal degeneration. The Retinal Pigment Epitheilium. 1978; 20:357.

LaVail MM. Circadian nature of rod outer segment disc shedding in the rat. Investigative Ophthalmology and Visual Science. 1980; 19:407. [PubMed: 7358492]

Li CM, Chung BH, Presley JB, Malek G, Zhang X, Dashti N, Li L, Chen J, Bradley K, Kruth HS, Curcio CA. Lipoprotein-like particles and cholesteryl esters in human Bruch's membrane: Initial characterization. Investigative Ophthalmology and Visual Science. 2005; 46:2576–2586. [PubMed: 15980251]

Malek G, Li CM, Guidry C, Medeiros NE, Curcio CA. Apolipoprotein B in cholesterol-containing drusen and basal deposits of human eyes with age-related maculopathy. The American Journal of Pathology. 2003; 162:413–425. [PubMed: 12547700]

McKechnie NM, King BC, Fletcher E, Braun G. Fas-ligand is stored in secretory lysosomes of ocular barrier epithelia and released with microvesicles. Experimental Eye Research. 2006; 83:304–314. [PubMed: 16563377]

O'Sullivan TN, Wu XS, Rachel RA, Huang JD, Swing DA, Matesic LE, Hammer JA 3rd, Copeland NG, Jenkins NA. dsu functions in a MYO5A-independent pathway to suppress the coat color of dilute mice. Proceedings of the National Academy of Sciences of the United States of America. 2004; 101:16831–16836. [PubMed: 15550542]

Ohbayashi N, Maruta Y, Ishida M, Fukuda M. Melanoregulin regulates retrograde melanosome transport through interaction with the RILP·p150Glued complex in melanocytes. Journal of Cell Science. 2012

Rachel RA, Nagashima K, O'Sullivan TN, Frost LS, Stefano FP, Marigo V, Boesze-Battaglia K. Melanoregulin, product of the dsu locus, links the BLOC-pathway and Oa1 in organelle biogenesis. PLoS One. 2012; 7:e42446. [PubMed: 22984402]

Rakoczy PE, Baines M, Kennedy CJ, Constable IJ. Correlation between autofluorescent debris accumulation and the presence of partially processed forms of cathepsin D in cultured retinal

pigment epithelial cells challenged with rod outer segments. Experimental Eye Research. 1996a; 63:159–167. [PubMed: 8983973]

Rakoczy PE, Lai MC, Vijayasekaran S, Robertson T, Rapp L, Papadimitriou J, Constable I. Initiation of impaired outer segment degradation in vivo using an antisense oligonucleotide. Current Eye Research. 1996b; 15:119–123. [PubMed: 8631199]

Rakoczy PE, Lai MC, Watson M, Seydel U, Constable I. Targeted delivery of an antisense oligonucleotide in the retina: Uptake, distribution, stability, and effect. Antisense & Nucleic Acid Drug Development. 1996c; 6:207–213. [PubMed: 8915505]

Rakoczy PE, Lai CM, Baines M, Di Grandi S, Fitton JH, Constable IJ. Modulation of cathepsin D activity in retinal pigment epithelial cells. Journal of Biochemistry. 1997; 324:935–940.

Rakoczy PE, Zhang D, Robertson T, Barnett NL, Papadimitriou J, Constable IJ, Lai CM. Progressive age-related changes similar to age-related maculardegeneration in a transgenic mouse model. The American Journal of Pathology. 2002; 161:1515–1524. [PubMed: 12368224]

Saftig P, Hetman M, Schmahl W, Weber K, Heine L, Mossmann H, Koster A, Hess B, Evers M, von Figura K. Mice deficient for the lysosomal proteinase cathepsin D exhibit progressive atrophy of the intestinal mucosa and profound destruction of lymphoid cells. The EMBO Journal. 1995; 14:3599–3608. [PubMed: 7641679]

Siintola E, Partanen S, Stromme P, Haapanen A, Haltia M, Maehlen J, Lehesjoki AE, Tyynela J. Cathepsin D deficiency underlies congenital human neuronal ceroid-lipofuscinosis. Brain. 2006; 129:1438–1445. [PubMed: 16670177]

Steinfeld R, Reinhardt K, Schreiber K, Hillebrand M, Kraetzner R, Bruck W, Saftig P, Gartner J. Cathepsin D deficiency is associated with a human neurodegenerative disorder. American Journal of Human Genetics. 2006; 78:988–998. [PubMed: 16685649]

Stewart SAA, Dykxhoorn DM, Palliser D, Mizuno H, Yu EY, An DS, Sabatini DM, Chen ISY, Hahn WC, Sharp PA, Weinberg RA, Novina CD. Lentivirus-delivered stable gene silencing by RNA in primary cells. RNA. 2003; 9:493–501. [PubMed: 12649500]

Tikellis G, Robman LD, Dimitrov P, Nicolas C, McCarty CA, Guymer RH. Characteristics of progression of early age-related macular degeneration: The cardiovascular health and age-related maculopathy study. Eye. 2007; 21:169–176. [PubMed: 16732219]

Urbanelli L, Emiliani C, Massini C, Persichetti E, Orlacchio A, Pelicci G, Sorbi S, Hasilik A, Bernardi G, Orlacchio A. Cathepsin D expression is decreased in Alzheimer's disease fibroblasts. Neurobiology of Aging. 2008; 29:12–22. [PubMed: 17049675]

Vetvicka V, Vektvickova J, Fusek M. Effect of human procathepsin D on proliferation of human cell lines. Cancer Letters. 1994; 79:131–135. [PubMed: 8019970]

Vetvicka V, Vetvickova J. Procathepsin D and cytokines influence the proliferation of lung cancer cells. Anticancer Research. 2011; 1:47–51. [PubMed: 21273579]

Woessner JF Jr. Specificity and biological role of cathepsin D. Advances in Experimental Medicine and Biology. 1977; 95:313–327. [PubMed: 596304]

Zaidi N, Maurer A, Nieke S, Kalbacher H. Cathepsin D: A cellular roadmap. Biochemical and Biophysical Research Communications. 2008; 376:5–9. [PubMed: 18762174]

Zarbin MA. Current concepts in the pathogenesis of age-related macular degeneration. Archives of Ophthalmology. 2004; 122:598–614. [PubMed: 15078679]

Zareparsi S, Buraczynska M, Branham KE, Shah S, Eng D, Li M, Pawar H, Yashar BM, Moroi SE, Lichter PR, Petty HR, Richards JE, Abecasis GR, Elner VM, Swaroop A. Toll-like receptor 4 variant D299G is associated with susceptibility to age-related macular degeneration. Human Molecular Genetics. 2005; 14:1449–1455. [PubMed: 15829498]

Zufferey R. Multiply attenuated lentiviral vector achieves efficient gene delivery in vivo. Nature Biotechnology. 1997; 15:871–885.

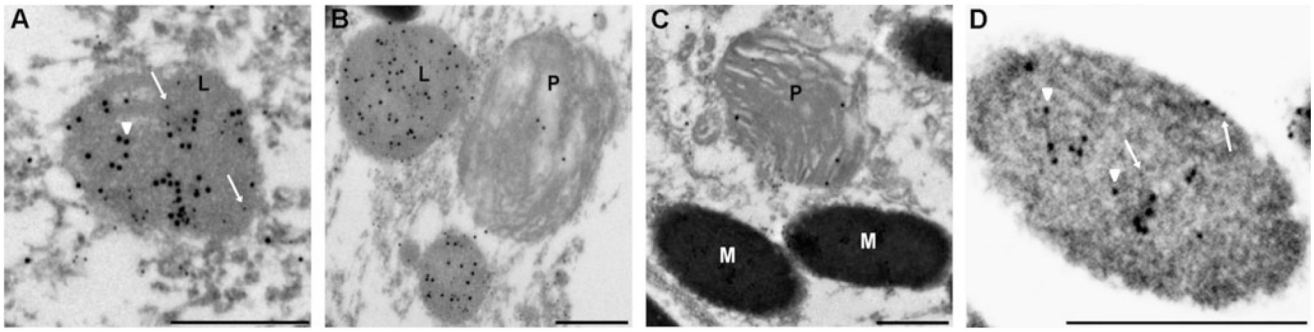

Fig. 1. MREG localizes to Cat-D containing vesicles

(**A** – **D**) Immuno-EM of MREG localization in RPE cells. Ultrathin sections obtained from LR White-embedded *Mreg*$^{+/+}$ mouse retinas were double-labeled with rabbit Cat-D polyclonal antibody and mouse MREG mAb165. Goat antirabbit IgG antibodies, conjugated to 15 nm gold particles, and antimouse IgG, conjugated to 10-nm gold particles, were used as secondary antibodies, respectively. Arrowheads indicate examples of Cat-D labeling (large particles), and arrows indicate examples of MREG label (small particles). Panel A. Labeling of a lysosome, L. Panel B. Labeling of lysosomes and a phagosome, P. Panel C, labeling of a phagosome and melanosomes, M. Panel D is a higher magnification of the melanosome on the left in panel C; the image has been made brighter so that the gold particles are evident against the darkly staining melanin. Scale bars = 500 nm.

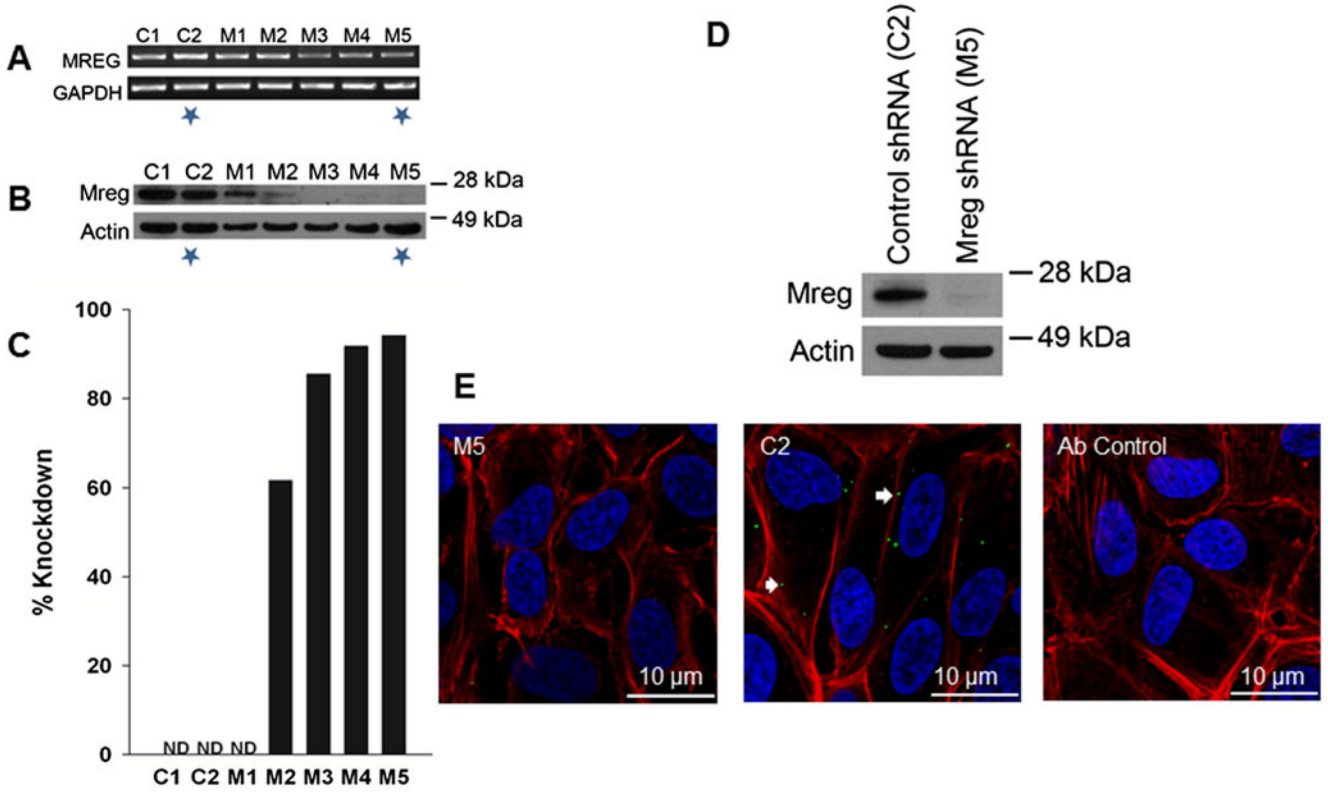

Fig. 2. Mreg shRNA gene silencing efficiency in ARPE19 cells

(**A**) Quantitation of MREG mRNA. RT-PCR products separated on agarose gels from five MREG lentiviral clones designated M1–M5, control shRNA with no shRNA insert (C1) and control shRNA containing nontarget shRNA (C2) demonstrating MREG shRNA knockdown efficiency. GAPDH is shown as an endogenous control. Stars indicate cells used in subsequent studies. (**B**) Immunoblot analysis showing MREG protein knockdown in shRNA ARPE19 cells. Actin is shown as a loading control. (**C**) Quantitation of % knockdown of MREG protein normalized to actin. (**D**) Immunoblot of control (C2) and MREG knockdown (M5) ARPE19 cells used for immunofluorescence. (**E**) Immunofluorescence localization of MREG in shRNA ARPE19 cells. Control (C2) and MREG knockdown (M5) ARPE19 cells were double labeled with anti-MREG mAb and 647-phalloidin (actin) Hoescht 33382. Bar, 10 μm.

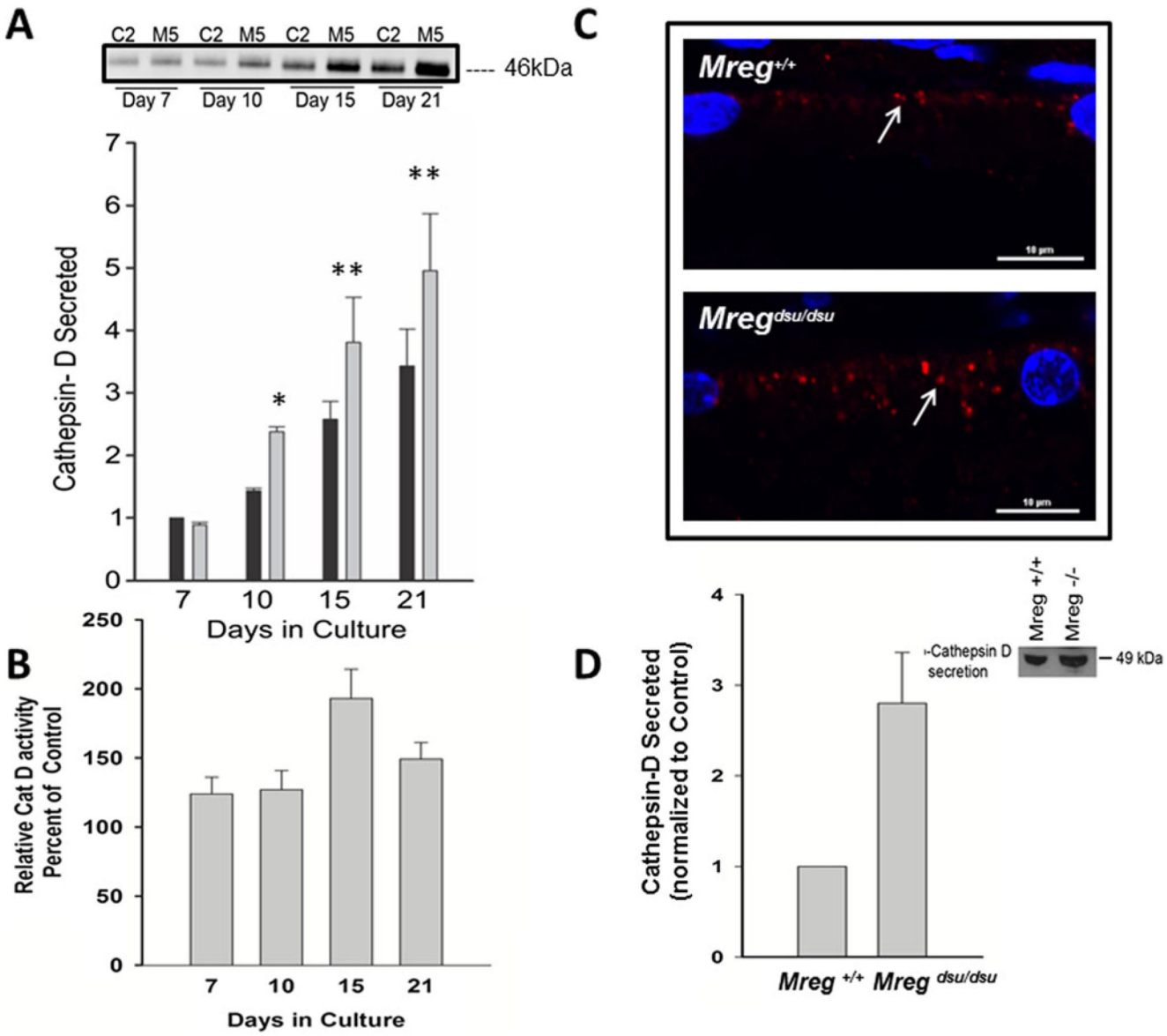

Fig. 3. Elevated Cat-D secretion in ARPE19 cells and primary cultures of *Mregdsu/dsu* RPE

(**A**) Conditioned media from basolateral side was collected from shRNA ARPE19 control (C2) and MREG (M5) knockdown cells after 7, 10, 15, and 21 days in culture and analyzed for Cat-D secretion. Cat D secreted is presented as mean ± SEM, n = 4. *Significantly different in M5 cells compared with controls (C2); at 10 days, P<01 and **significantly different at 15 and 21 days, P<0.05. (**B**) Cat-D activity (units/ml) in conditioned media from C2 and M5 cells after 7, 10, 15, and 21 days in culture. Presented as mean ± SEM, n = 3. *Activity is significantly different at all time points, P <0.05. (**C**) Cat-D labeling in eyecups isolated from 4-month old *Mreg*$^{dsu/dsu}$ and *Mreg*$^{+/+}$ mice. This is a representative image (two animals, four eyes, assessment of 10 areas in each eye). (**D**) Quantitation of pro-Cat D secretion from primary RPE cells extracted from 6-week old *Mreg*$^{+/+}$ and *Mreg*$^{dsu/dsu}$ mice. Inset, Western blot of data shown in **D**.

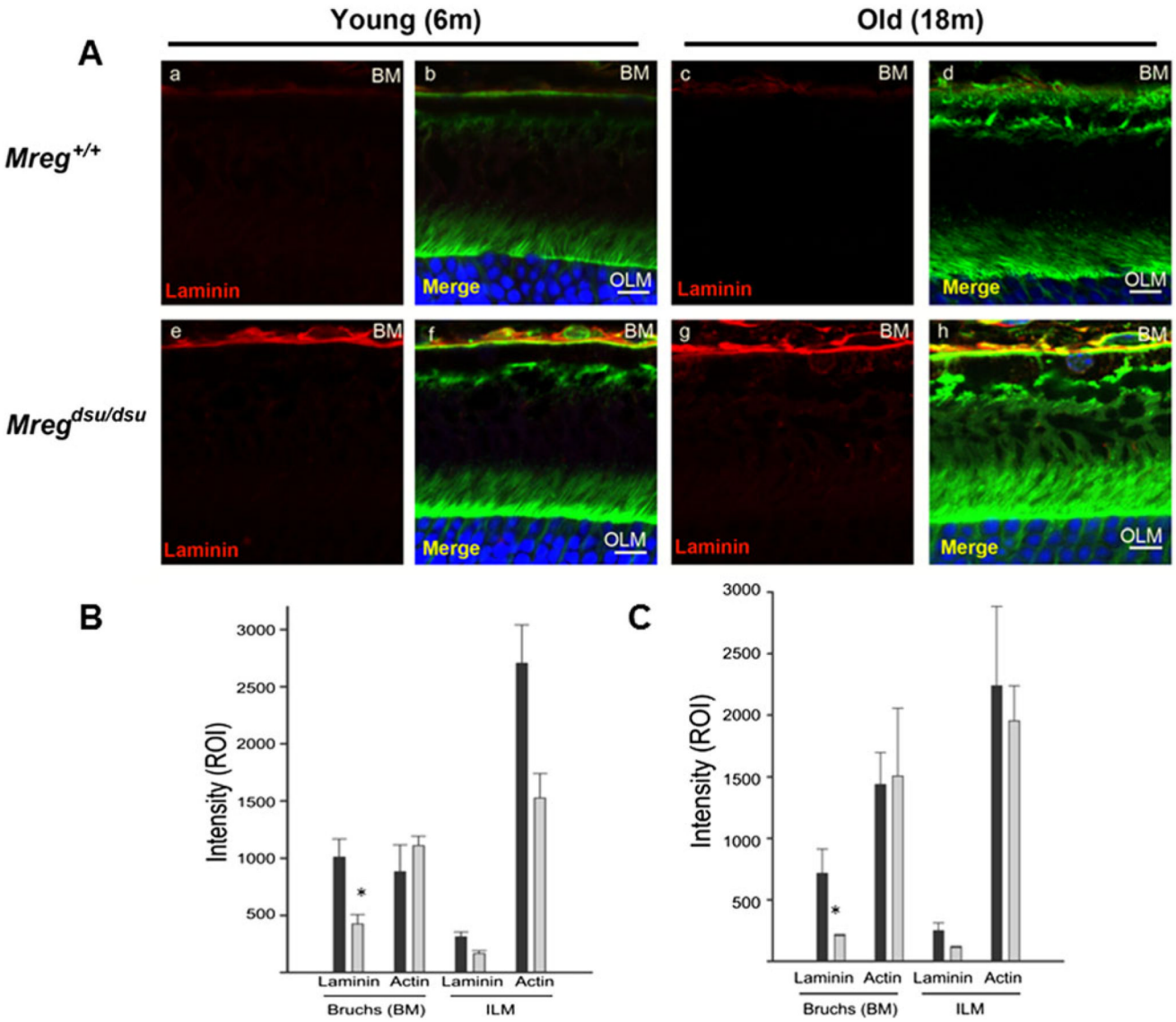

Fig. 4. Increased laminin in Bruch's membrane in *Mregdsu/dsu* mice

(**A**) Immunofluorescence analysis of laminin in eyecups isolated from young (6 months) and old (18 months) *Mreg*$^{dsu/dsu}$ and *Mreg*+/+ mice. Panels a, b: *Mreg*$^{+/+}$6 m; Panels c, d: *Mreg*$^{+/+}$18 m; Panels e, f: *Mreg*$^{dsu/dsu}$6 m; Panels g, h: *Mreg*$^{dsu/dsu}$18 m; Nuclei are stained with Hoescht 33258 and sections counterstained with phalloidin (actin) bar, 10 μ m. (**B**) Analysis of laminin levels in 6-month old animals. ROI of laminin in area of BM and OLM (as control). Values are average from four animals, four eyes and assessment of 10 areas in each eye. *Significant difference between *Mreg*$^{dsu/dsu}$ and *Mreg*+/+ mice of laminin in BM, P <0.05. (**C**) Analysis of laminin levels in 18-month old animals. ROI of laminin in area of BM and OLM (as control). Values are average from four animals, four eyes, and assessment of 10 areas in each eye. *Significant difference between *Mreg*$^{dsu/dsu}$ and *Mreg*$^{+/+}$ mice of laminin in BM, P <0.05.

Table 1

Cell lysis

	Lactate dehydrogenase activity			
	Day 1	**Day 3**	**Day 7**	**Day 10**
C2 (Control)	60.1 ± 9.90	51.7 ± 5.30	114.1 ± 5.6	333.4 ± 22.4
M5 (MREG KD)	53.8 ± 11.3*	64.5 ± 5.40*	115.2 ± 16.8*	324.8 ± 36.2*

Lactate dehydrogenase activity, expressed as mUnits/ml, was determined in conditioned media isolated from C2 and M5 cells at the indicated time points. Results are an average of four analyses ± SEM.

*$P < 0.050$.

Table 2

Normalized Cat-D activity

	Normalized Cat-D activity			
	Day 7	**Day 10**	**Day 15**	**Day 21**
C2 (Control)	0.178 ± 0.026	0.148 ± 0.016	0.043 ± 0.002	0.042 ± 0.006
M5 (MREG KD)	0.225 ± 0.035**	0.116 ± 0.011*	0.082 ± 0.004*	0.062 ± 0.003**

Degradation of a fluorogenic Cat-D substrate was measured in basolateral conditioned media isolated from C2 and M5 cells at the indicated time points. Activity was normalized to Cat-D protein as determined by quantitative Western blots. Results are an average of three experiments ± SEM.

** $P > 0.100$ for days 7 and 21,

* $P < 0.05$ for days 10 and 15.